

Demonstrated Low Pressure Loss Inlet and Low Equivalence Ratio Operation of a Rotating Detonation Engine (RDE) for Power Generation

Alexander R. Baratta^{1*} and Jeffrey B. Stout^{2*}
*Aerojet Rocketdyne, Canoga Park, CA 91304

A large scale rotating detonation engine (RDE) combustor was recently tested using natural gas and air with the objective of demonstrating feasibility of using pressure gain combustion (PGC) as a method to enhance the efficiency of power generation. 195 tests were conducted with 22 different hardware combinations of a 13.4" scale RDE. Flowrates up to 24 lbm/sec and combustor pressures up to 204 psia were achieved. An inlet/injector was tested which allowed sustained detonation combustion with less than 7% pressure loss from manifold to combustor. In addition, a tailored injection scheme allowed overall detonation combustor operation while maintaining a low fuel equivalence ratio. A plant system model was used to show that low inlet pressure loss and low equivalence ratio RDE operation can result in 66% net plant power generation efficiency.

I. Introduction

One method of realizing pressure gain combustion is to harness the energy produced during a detonation combustion cycle. Opposed to deflagration combustion, which occurs at a constant total pressure, detonation combustion can increase the total pressure of a system. Detonation waves operate as both a shock and reaction front passing through mixed propellants. The shock compression induces an elevated pressure and temperature immediately before the combustion reaction occurs. Under these conditions the reaction takes place at a higher total pressure, yet releases the same amount of thermal energy into the system. The result is an exhaust flow with more energy content available for usable work. Developing a device able to support detonation and harness this usable energy has become an engineering challenge. One device of particular interest in the field is the rotating detonation engine (RDE). An RDE provides several advantages with respect to similar pressure gain combustion devices, including reduced complexity and providing near steady combustor exit conditions. It works by supporting one or several sustained detonation waves that travel around an annular combustion chamber. After a wave passes, fresh propellants are mixed and injected prior to the arrival of the next wave. Despite its advantages, many technical challenges still exist before pressure gain combustion can be realized in a practical rotating detonation engine.

An Aerojet Rocketdyne (AR) program was funded by the National Energy Technology Laboratory (NETL), part of the U.S. Department of Energy, to evaluate the benefits of an RDE in a turbine power plant system. Efforts led by AR were subcontracted to Southwest Research Institute, the University of Alabama, the University of Michigan and Purdue University. These efforts all contributed to the experimental design, diagnostic techniques and test approach for a large engineering scale RDE combustor. The combustor was designed to be modular such that a variety of conditions could be tested including changing geometries at the chamber inlet and exit. Over a six month period twenty two different hardware configurations recently tested at Purdue University's Zucrow labs under a variety of flow conditions. With the goal of evaluating an RDE in a turbine system, the total pressure recovery through the

¹ Component Product Engineer, Combustion Devices, AIAA Member.

² Chief Engineer, Advanced Combustion Devices, AIAA Member.

entire system became the metric for evaluating performance. Total pressure recovery was influenced by both total pressure gain through the detonation process, and static pressure losses induced by hardware geometry and flow conditions. Both phenomena were evaluated for individual tests, and analyzed under the scope of the entire campaign. While pressure gain was never directly measured in the system, a total pressure loss of less than 7% was achieved using low pressure loss inlet hardware. This configuration avoided substantial static pressure losses in the test article while still maintaining sustained detonation behavior. This result, as well as other unexpected phenomena, demonstrated substantial efficiency gains in a modeled turbine power plant system.

II. Experiment Description

A. Hardware Review

The rotating detonation engine evaluated in this test campaign utilized modular hardware that could be interchanged between tests. Different hardware configurations allowed testing of a variety of inlet geometries, injection conditions, and exit conditions. Photographs of the complete RDE assembly are shown in Figure 1.

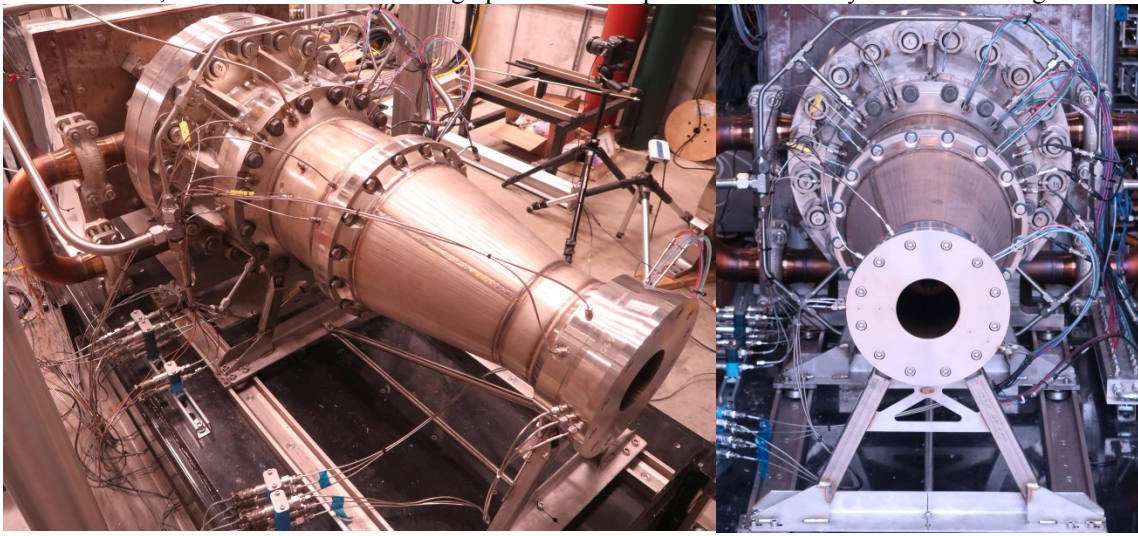


Figure 1 Photographs of the assembled RDE attached to the test stand.

The RDE test article included an air manifold adapter to attach it to the APEX test stand at Purdue University's Zucrow Labs. Prior to entering the engine's annular combustion chamber, the air flow passed through a modular air inlet and fuel injection assembly. The geometry of this region in the test article varied considerably depending on the hardware configuration, but always encouraged efficient mixing of the fuel and air flow for optimal detonation. The air inlet and fuel injection assembly had a secondary task of reducing the effect of downstream pressure fluctuations on the conditions in the air manifold. After injection, the fuel and air mixture entered an annular combustion chamber where the cyclical detonation process occurred. The chamber had a diameter of 13.3" and axial length of 12.25". A variety of outlet hardware, including a large diffuser, was used to control the exhaust flow beyond the combustion chamber. Effective detonation air and hydrocarbon fuel in an RDE requires backpressure in the chamber, thus each outlet assembly included a bluff faced nozzle to choke the flow. Choked flow was also required in order to determine the system's pressure gain performance using the equivalent available pressure method explained later. The system was designed to accommodate rapid disassembly and reassembly of diverse hardware configurations. Figure 2 displays a cross sectional rendering of the assembled test article on the test stand.

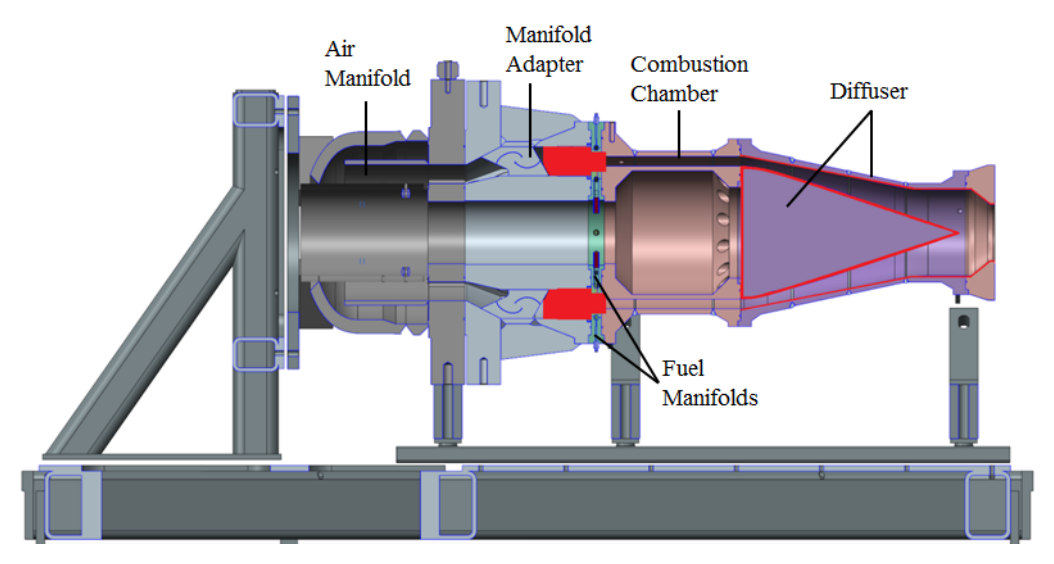


Figure 2 Cross sectional rendering of assembled test article. ITAR sensitive geometries have been covered in red.

Twenty two different hardware configurations were used in the test article during the engineering scale test campaign. Each configuration provided a unique path through the engine and induced a variety of phenomenon on the flow itself.

All tests used two separate manifolds to inject fuel from both the interior and the exterior of the annulus. The two injectors could be independently aimed upstream or downstream with respect to the airflow. The position of the fuel injectors could be independently moved along the engine axis upstream or downstream of the air inlet "choke" point, where the inlet reached is minimum flow area. These degrees of freedom allowed for a wide variety of conditions under which fuel was injected into the air flow. In addition to changing the direction and location of fuel injection, the geometry through which the flowing air entered the combustion chamber was also varied. The region leading up to the inlet was subject to soft and sharp corners in some cases, or a gradual taper in others. The location and magnitude of the minimum flow area was also changed in different hardware configurations. Unique geometric contours were positioned in front or behind this "choke" point to further alter the flow. It has been previously determined that the ratio between the minimum flow area and the chamber flow area, or "inlet area ratio," is a valuable number in producing and qualifying sustained detonation behavior, thus a variety of ratios were explored. Each inlet configuration produced unique behavior that affected the propellants mixing efficiency and propensity to detonate.

The exhaust exit flow area ratio was also changed during the test campaign. As stated earlier, in order for detonation to be sustained there must be backpressure in the combustion chamber. In the case of an RDE, converging nozzles are generally used to maintain this backpressure for the duration of its firing. Higher average combustion pressures also allow better traceability to potential operation in a high pressure power generating turbine. All hardware configurations evaluated used converging nozzles at the end of the test article to sustain detonation in the system. It has been previously determined that the ratio between the flow area in the combustion chamber and the smallest flow area of the nozzle, or "nozzle area ratio," is a valuable number in producing and qualifying sustained detonation behavior. Therefore, several different ratios were used during the test campaign to provide insight as to how each affected system performance. In addition to different nozzle hardware, a diffuser assembly was used during portions of the testing. The diffuser assembly consisted of an outer shell that attached to the outer portion of the combustion chamber, and an inner, cone shaped center body that attached to the interior of the combustion chamber. The purpose of the diffuser was to help convert the rapid pressure fluctuations produced during detonation into useful total pressure rather than lose this energy to entropy through viscous mixing phenomena. The contours of the diffuser were carefully designed based on previous test results, as well as predictions from computational fluid dynamics (CFD) analysis to best accomplish this goal. The end of the diffuser included an interchangeable nozzle that allowed for various area ratios to be tested. Although a variety of tests were executed without the diffuser, the majority of the discussion in this paper surround testing that included the assembly. The test article including the diffuser assembly can be seen in both Figure 1 and Figure 2.

As mentioned earlier, it was necessary to have a bluff face at the end of the test article in order to accurately evaluate system performance. Using the equivalent available pressure (EAP) method for calculating pressure gain,

thrust is the most significant measurement. Any hardware beyond the smallest choke point of the nozzle would affect the measured thrust, thus a bluff face simplifies the calculations. The configurations with and without the diffuser assembly met this bluff face requirement. Additionally, the two nozzles used with each of these configurations were designed to have the exact same area ratios to allow for direct comparison. Configurations that included the center body of the diffuser, but not the outer shell, did not meet the bluff face criteria. Tests that used this configuration could not be accurately evaluated for pressure gain. This configuration also did not match area ratios of the other two.

The performance of each unique hardware configuration was evaluated with respect to the resultant measured detonation behavior in the combustion chamber and overall system pressure gain. Different hardware configurations proved to have a substantial effect on the system performance throughout the test campaign and often produced unexpected results. Table 1 and Table 2 summarizes all of the hardware configurations used during the test campaign.

Inlet Hardware	1	2	3	4	5	6	7	8	9	10
Inlet Area Ratio (Ai/Ac)	3.73	3.73	3.73	10.1	3.996	1.74	3.88	2.96, 3.64, 2.88	3.93, 2.06	1.74
Injection Direction	Outer Downstream, Inner Upstream	Outer Downstream, Inner Upstream	Outer Upstream, Inner Downstream	Downstream	Outer Downstream, Inner Upstream	Upstream	Downstream	Downstream	Upstream	Upstream
Injection Position	Before Minimum Area	Before Minimum Area	After Minimum Area	After Minimum Area	Before Minimum Area	Before Minimum Area	After Minimum Area	After Minimum Area	After Minimum Area	Before Minimum Area
Date Range	12/17/2018 - 12/18/2018	12/19/2018 - 12/20/2018	1/23/2019 - 1/24/2019, 1/28/2019 - 1/31/2019	1/25/2019	3/27/2019 - 4/1/2019, 5/1/2019 - 5/15/2019	4/3/2019, 4/23/2019		3/21/2019 - 3/25/2019	4/5/2019 - 4/17/2019	4/19/2019

Table 1 Inlet hardware configurations used during test campaign.

Table 2 Exit hardware configurations used during test campaign.

Exit Hardware	А	В	С
Nozzle Description	annular backpressure ring and flat center plate	outer diffuser and centerbody with downstream nozzle	annular backpressure ring and diffuser centerbody
Nozzle Area Ratio (An/Ac)	2.0, 2.5	2.0, 2.5	1.74, 2.01

B. Facility and Conditions

The engineering scale RDE engine was tested at Purdue University's Zucrow Labs. The engine utilized air and supplemental O2 as its oxidizer and natural gas as its fuel source. The air flowed from a high pressure tank and passed through a large heater before being metered by a critical flow venturi nozzle. The heater temperature and regulated pressure controlled the conditions of the air flow seen by the engine. During the campaign, the air manifold saw temperatures between 555 and 862 °F, pressures between 42.3 and 258 psia, and mass flow rates between 22 lbm/s and 4.7 lbm/s. During tests where supplemental oxygen was included, the oxygen was injected after the air venturi nozzle, but upstream of the air manifold. This location encouraged uniform mixing before entering the engine, yet consistent control of the air mass flow rate. The oxygen flow rate was also metered by a critical flow venturi nozzle.

The natural gas fuel was sourced from the local natural gas line and its composition is taken as a monthly average of the mole fraction of the major species reported by the distributor. As discusser earlier, two separate fuel lines and manifolds were used to inject fuel from both the interior and exterior walls each controlled by separate venturi nozzles. The inner fuel manifold saw temperatures between 14 and 570 °F, pressures between 118 and 680 psia, and mass flow rates between 0.09 and 0.85 lbm/s during testing. The outer fuel manifold saw temperatures

between 16 and 422 °F, pressures between ambient and 652 psia, and mass flow rates between 0 and 0.8 lbm/s during testing.

Upstream pressure and temperature measurements were monitored throughout each test to compute mass flow rates for individual propellants.

Over the test campaign, the variety of conditions provided a range of results. The average chamber pressure was measured between 25 and 204 psia with a total propellant mass flow rate between 5.7 and 24.4 lbm/s. Thrust was measured as high as 3567 lbf.

C. Instrumentation

The test article instrumentation was localized to 4 axial locations on the test article. These locations were 1.25", 5.5", 10.22", and 31.5" downstream of the inlet minimal choke point respectively. Locations 1 through 3 spanned the length of the annular combustion chamber to identify trends as the flow moved downstream. Location 4 was positioned at the end of the diffuser assembly to asses flow conditions after diffusion, just prior to exiting the article.

Several pressure sensors were placed at each axial location on the engine. For low speed data acquisition, a normal static pressure tap and a transducer in the Capillary Tube Attenuated Pressure (CTAP) configuration each sampling at 1 kHz were placed at each location 1 through 4. An additional static pressure tap and thermocouple were included on the air and fuel manifolds to measure the conditions before entering the engine. With regards to high speed data acquisition, two water cooled piezoelectric transducers (PCB® 113B24) with inline charge amps (422E12) sampling at 1 MHz measured chamber pressure oscillations at location 1 with a 22.5 degree circumferential offset. This offset allowed for identification of steady, circumferential wave movement as the detonation waved passed from one sensor to the next. Additional PCBs operated at locations 3 and 4, as well as one in the air manifold. The aperture for the PCBs was 0.0625" in diameter with a depth of 0.08" and a diaphragm width of 0.217". Thrust measurements of the engine were made using a single component horizontal thrust stand provided by Force Measurement Systems®. It utilized an Interface® 2000-D-10K-4-U load cell. An unforeseen offset was identified in the thrust measurement system caused by the thermal expansion of the air supply line. An adjustment factor was individually calculated using flow conditions prior to ignition and applied to each test. This adjustment factor was verified using auxiliary tests conducted on the test stand.

A series of tests utilized the unique particle image velocimetry (PIV) abilities of the Purdue Zucrow labs. A pulse-mode Spectral Energies QuasiModoTM laser was used to generate 100 kHz doublets in concert with a Vision Research Phantom v2512 high speed camera for PIV measurements. The air was seeded with 200 nm Zirconia particles as it was introduced into the air manifold. The resulting velocity vectors produced by the PIV were used to anchor various analytical and CFD models. Figure 3 shows a photograph of the laser operating on the RDE engine during successful firing. In this test the test article is assembled without the outer diffuser shell, but with the center body (exit hardware configuration C).

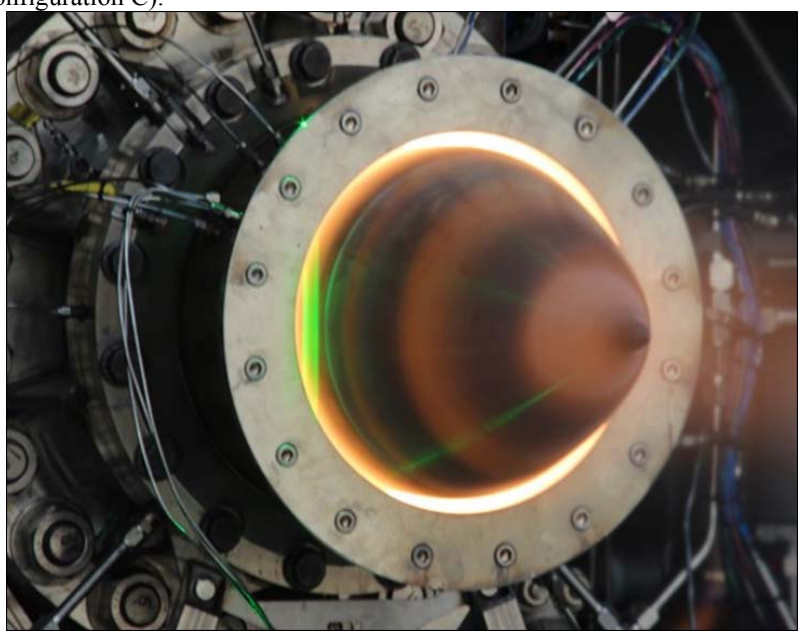


Figure 3 Test article hot firing with PIV laser visibly operating along combustion chamber exit.

III. Results and Discussion

A. Total Pressure Calculations

With respect to the program goals, achieving pressure gain was of top priority. In an RDE based power plant system the total pressure available to drive a downstream turbine is the most significant factor in evaluating plant efficiency. For this reason, system performance of each test was calculated with respect to its pressure recovery. The metric used to evaluate the system performance during a test was the equivalent available pressure (EAP) based on the method put forth by Kaemming and Paxson [1]. In their procedure the pressure at the device exit throat (assumed to be sonic) P_8 is computed from the thrust F_g , the throat area A_g , and the base pressure P_0 .

$$P_8 = \left(\frac{F_g}{A_8} - P_0\right) / (\gamma + 1) \tag{1}$$

The system's equivalent available pressure at the exit is calculated by isentropically expanding the throat pressure to ambient conditions.

$$EAP = P_8 \left(\frac{\gamma + 1}{2}\right)^{\frac{\gamma}{\gamma - 1}} \tag{2}$$

The EAP represents the pressure available for useful work remaining in the flow. The EAP is then compared to the air manifold pressure to evaluate pressure gain in the system. This comparison takes into account all parts of the test article, including the inlet and injector, when measuring pressure gain. EAP also requires a bluff end on the system with no nozzle coefficient effects for accurate calculations. Using this method, thrust became the most important measurement in evaluating the performance of the system. Pressure gain was never directly measured during the test campaign; however Table 3 characterizes the performance of a select series of significant tests with respect to the critical measurements.

Table 3 Thrust measurements and associated EAP pressure gain for significant tests.

Date	Test#	Detonation Score	Propellant Total Flowrate (lbm/sec)	Air Manifold Pressure (psia)	Thrust, net (meas.) (lbf)	Adjusted Thrust (lbf)	EAP	Pressure Gain
2019-04-03	002	6.2	17.58	155.46	2043	2807	147.15	-5.35%
2019-04-03	004	6.2	14.61	130.26	1555	2317	123.52	-5.18%
2019-04-23	006	8.0	16.75	152.54	1512	2301	150.46	-1.36%
2019-04-23	009	8.0	17.00	166.05	1732	2459	159.97	-3.66%
2019-05-14	005	7.0	14.11	153.48	1356	2251	120.35	-21.59%
2019-05-15	004	9.4	14.12	155.05	1407	2246	*120.65	-22.19%

^{*}EAP measurement with unknown uncertainty because diffuser center body included on assembly.

Note: The detonation score criteria were developed by Jeffrey Stout based on measured detonation wave conditions. The direct criteria can be seen below.

0	No combustion
1	combustion, zero sign of detonation behavior
2	brief hint of wave-like activity
3	intermittent wave-like activity
4	Consistent wave-like activity, occasional slapping mode
5	Slapping mode, weak, occasional break down to wave-like activity
6	Slapping mode, consistent thru run, Mach 2 minimum
7	Strong slapping mode, often jumps to one-directional waves
8	Mostly one-directional wave(s), occasional reversal or slapping mode
9	One-directional wave(s), consistent thru run, <85% CJ velocity
10	One-directional wave(s), high contrast wave front, high pressure, consistent thru run, >85% CJ velocity

B. Strong Detonation Behavior

The testing conducted on May 14th and May 15th provided some of the best detonation behavior seen during the test campaign. More specifically, test 5 on May 14th and test 4 on May 15th were identified as the strong examples of detonation behavior for this campaign. The behavior in these cases can be attributed to both the hardware configuration used and the flow conditions provided to the test article. On both these dates inlet hardware configuration 5 was used. Figure 4, Figure 5, Table 4, and Table 5 characterize the wave behavior for these two tests.

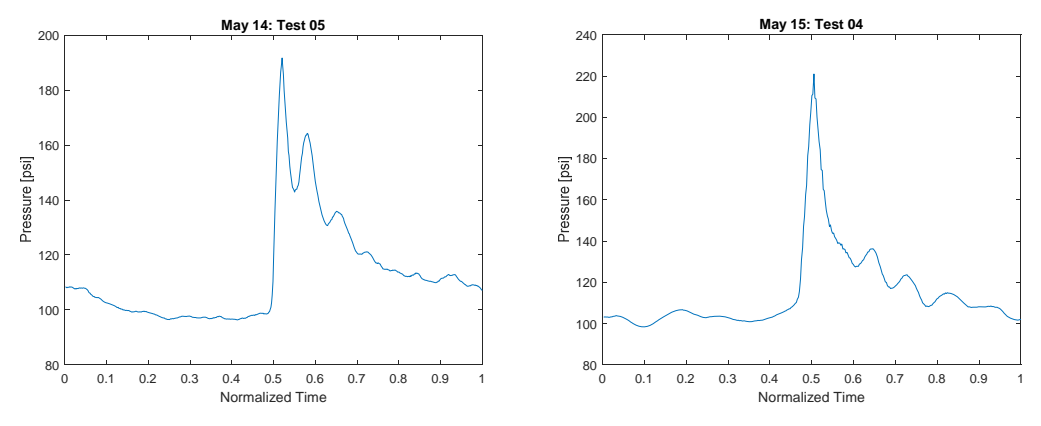


Figure 4 Average wave shapes for optimal detonation tests.

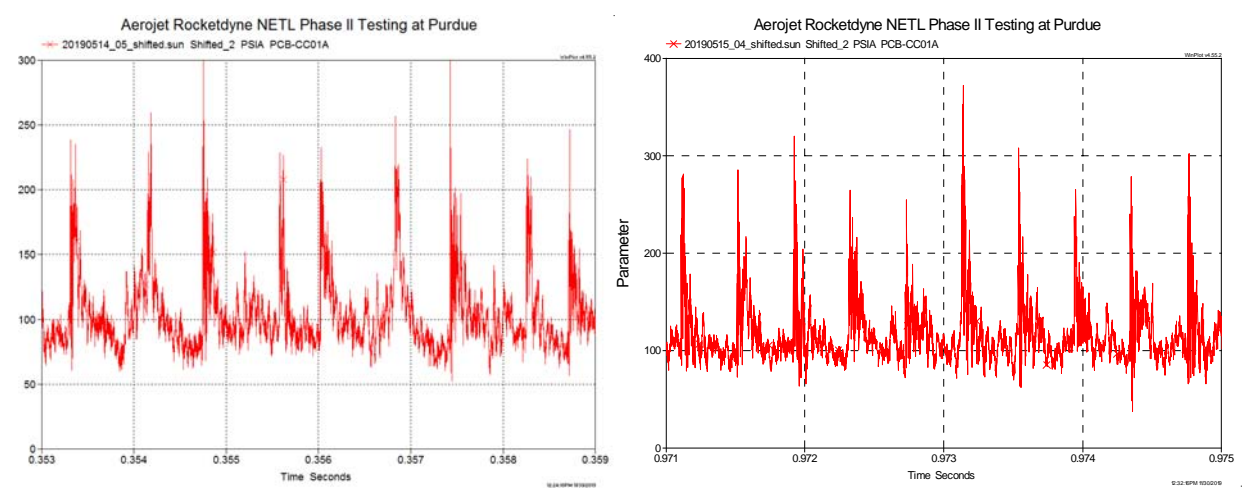


Figure 5 Raw pressure data of detonation waves measured during test 5 on 5/14 (top) and test 4 on 5/15 (bottom).

Figure 4 displays the average wave shape of the detonation wave taken over a specified time period of the test. Due to the noisy nature of detonation waves passing by a PCB, a composite average provides a smoother, clearer picture of wave behavior in the engine. Figure 5 is the raw pressure trace measured in the engine. In addition to an averaged shape, the raw trace is necessary to identify any features that could be lost through the averaging process.

Table 4 Average and peak pressure spikes measured along axis of engine.

Date	Test #	Press Spike Range Average, Location 1	Press Spike Range Peak, Location 1	Press Spike Range Average, Location 1	Press Spike Range Peaks, Location 1	Press Spike Range Average, Location 3	Press Spike Range Peaks, Location 3	Press Spike Range Average, Location 4	Press Spike Range Peaks, Location 4
5/14/2019	005	290	330	308	350	257	280	75	86
5/15/2019	004	350	400	300	345	120	130	N/A	N/A

Table 4 identifies the detonation pressure spikes measured at the previously defined locations on the engine. An average pressure spike metric and peak pressure spike metric were both recorded. The peak pressure spike metric was based on an approximate process of averaging the top 10% of pressure spikes.

Table 5 Performance values of detonation waves during tests.

*Peak measurements with previously described aperture

Date	Test #	Chamber Pressure (psi)	*Average Peak (psi)	*Average Peak to Satic Pres. Ratio	Dominant Freq (Hz)	Number of Waves	Wave Speed (m/s)	Ratio Actual to CJ Velocity			
5/14/2019	005	102	299	2.94	1120	1	1198	66.3%			
5/15/2019	004	115	325	2.83	2475	2	1323	70.8%			

Note: CJ Velocity is the Chapman Jouguet velocity as calculated using the NASA Chemical Equilibrium with Applications program (CEA) and the measured test conditions.

As seen in Figure 4 and Figure 5, for both cases the detonation spikes are very sharp from the static plateau as would be expected. From Table 4 and Table 5 we see in test 5 the detonation pressure spikes could be as high as 343% of the static pressure, but on average were around 294%. In test 4 the detonation pressure spikes were seen as high as 347% of the static pressure, but on average were around 283%. The measurements do not compensate for attenuation, and thus could be higher.

From Figure 4 and Figure 5 it was determined that the detonation behavior in test 4 was better than that of test 5. While the magnitude of the spikes in these two tests is proportionally very similar, the shape of the pressure spike from test 4 is smoother and more consistent. Test 4 does show some fluctuations in pressure after the detonation spike, but the peaks and fluctuations following the detonation spike in test 5 are more substantial. It also takes longer for the pressure to reach a static value in test 5 than in test 4 after the detonation wave has passed. These irregularities in the wave shape indicate inconsistencies in the detonation behavior. It can also be seen from Table 5 that the detonation waves in test 4 were substantially faster than the waves in test 5, and thus closer to the Chapman Jouguet velocity. The comparison between test 5 and test 4 is important because different hardware configurations were used on May 14th and May 15th. While the inlet/injection hardware remained the same, the outer diffuser was attached to the engine on May 14th (exit hardware configuration B), but not on May 15th (exit hardware configuration C), although the exit area ratios were nearly identical. Taking a look at Figure 4, this would seem to indicate that the test article was less supportive of optimal detonation behavior when the outer diffuser was attached. While this wasn't the purpose of the diffuser, a comparison between the diffusers advantages and disadvantages to system performance could be useful in the future. While these two test cases provide just a single example, this trend persisted throughout test campaign.

Taking a look at these tests with respect to the rest of the testing in the campaign, several important trends appeared. In general, inlet configurations with higher area ratios produced better detonation behavior. Both test 5 on May 14th and test 4 on May 15th had relatively high area ratios with respect to the rest of the hardware. This phenomenon can be explained due to stronger choking at the inlet region. Stronger choking before entering the combustion annulus leads to greater turbulence in this region and thus better mixing between fuel and air. Stronger choking also increases the pressure drop between air manifold and combustion annulus. With regards to evaluating pressure recovery, this inlet pressure drop can be one of the biggest factors detracting from potential pressure gain. Under the assumption that stronger detonation leads to better pressure recovery after combustion, the challenge of the program was to achieve strong detonation behavior with a low pressure drop through the inlet/injection region [2].

C. Low Pressure Drop Detonation

The two tests performed on April 3rd achieved both sustained detonation behavior and a low pressure drop through the air inlet. The engine configuration for these two tests utilized the full diffuser assembly (exit hardware configuration B) on the engine as well as the smallest inlet area ratio. The inlet geometry saw fuel injection aimed upstream, and positioned before the smallest flow area (inlet hardware configuration 6). The geometry itself an air flow path with a taper in to a minimum cross sectional area, followed by an expansion taper to the combustion annulus flow area. As stated previously, this minimum area was large in comparison to the rest of the inlet hardware configurations tested. Figure 6 shows the static pressure traces measured during a nominal test during the campaign.

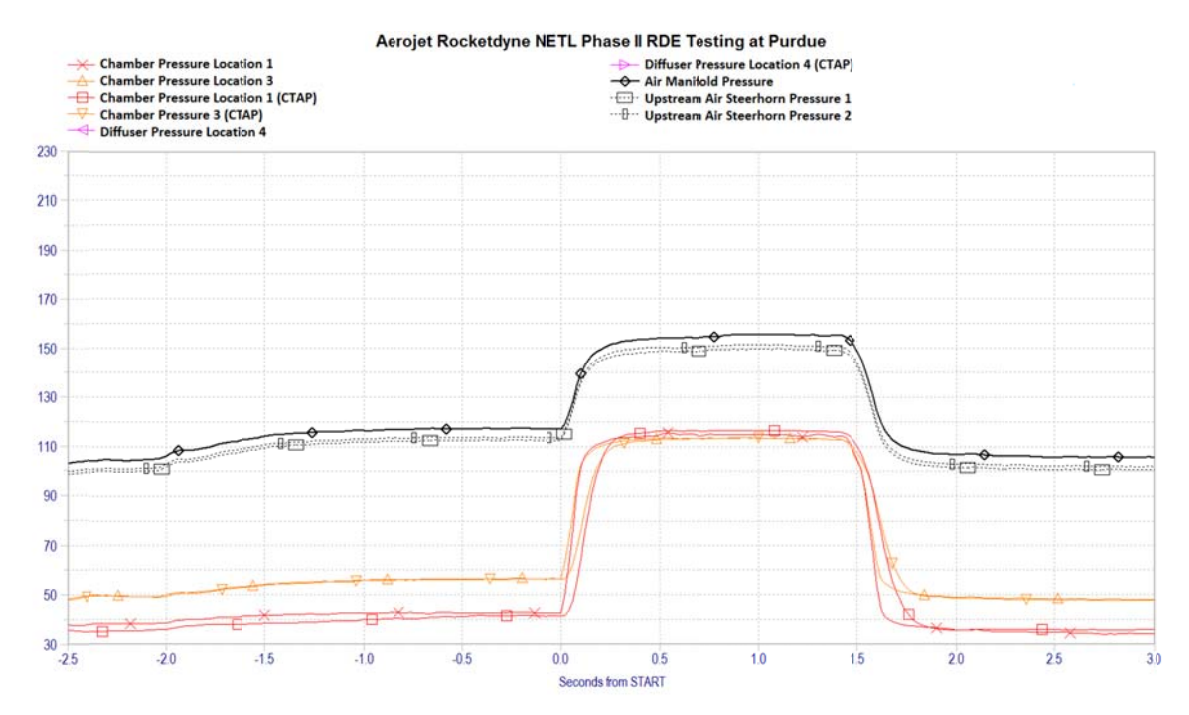


Figure 6 Plotted traces of the low speed pressure sensors over the duration of test 4 on 5/15.

Note: The steerhorn is essentially part of the test stand's air manifold upstream of the test article's air adapter. The flow velocity and pressure difference between the steerhorn, air manifold and the air adaptor were negligible and therefore could be reasonably treated as one volume.

There is an obvious and substantial drop in static pressure between the air manifold and chamber caused by inlet geometry choking the flow. In this case, the pressure loss between the air manifold and the chamber was measured at around 31%. Losses such as this were generally the largest total pressure loss throughout the system seen during testing. Figure 7 shows the static pressure traces measured during the low pressure loss test.



Figure 7 Plotted traces of the low speed pressure sensors during test 2 on 4/3.

Note: In test 2 the air manifold pressure sensor appears to malfunction at around 0.75 second as it stops tracking the air steerhorn pressures and dips below chamber pressure.

The pressure loss between the air manifold and the chamber was measured at less than 10% during low pressure loss testing. This is significantly smaller than all other tests during the campaign. Due to the inlet hardware geometry, the flow remains subsonic as it passes from the manifold into the chamber. Without a choke, viscous and shock losses in total pressure were largely avoided [2].

Characterization of the detonation behavior during the low pressure loss tests can be seen below.

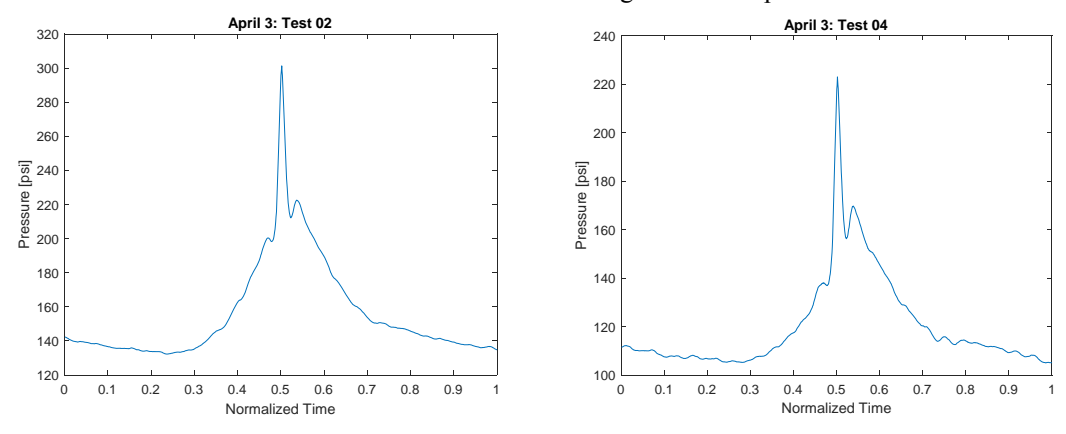


Figure 8 The normalized average shape of the pressure cycle as a detonation wave passes by a PCB during the low pressure loss testing on 4/3. This is an average of all waves over a 0.1 second period.

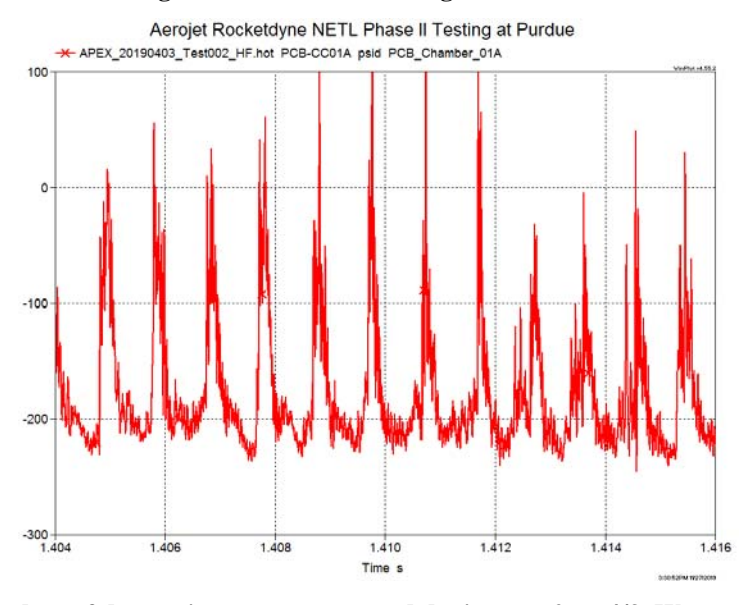


Figure 9 Raw pressure data of detonation waves measured during test 2 on 4/3. Wave traces measured during test 4 on 4/3 are comparable.

Figure 8 and Figure 9 show the averaged and raw pressure traces of the detonation waves measured during the low pressure loss testing. Compared to the strong detonation cases discussed above, the low pressure drop wave traces do not follow the same trends traditionally expected from detonation waves. Rather than undergoing an abrupt, steep pressure spike from the static pressure plateau, these traces exhibit a slower increase in pressure prior to the detonation spike, as well as a slower decrease to static pressure after. This behavior is theorized to be due to parasitic deflagration occurring in the chamber prior to the arrival of the circling detonation wave and commensurate deflagration occurring after its passed [3]. In these cases the relatively slower detonation wave is taking longer to reach the fresh propellants in the annulus, and therefore they begin undergoing deflagration prior to its arrival. This deflagration causes a slow increase in pressure prior to the arrival of the detonation wave. Table 6 characterizes the speed and strength of the measured waves.

Table 6. Characteristics of measured detonation waves during the low pressure loss testing on 4/3.

*Peak measurements with previously described aperture

Date	Test #	Chamber Pressure (psi)	*Average Peak (psi)	*Average Peak to Satic Pres. Ratio	Dominant Freq (Hz)	Number of Waves	Wave Speed (m/s)	Ratio Actual to CJ Velocity
4/3/2019	002	141	303	2.14	1020	1	1091	56.5%
4/3/2019	004	116	223	1.92	1020	1	1091	56.2%

Table 6 shows that the waves measured during the low pressure drop are notably slower and weaker than the waves measured during the strong detonation behavior tests. There are several potential reasons for this, including poorer mixing in the flow. Without a choking region to encourage turbulence or recirculation regions, the fuel and air flows may not have an opportunity to mix efficiently. Another reason could be due to chamber pressure fluctuations permeating upstream to affect inlet and manifold conditions. A choking region at the inlet acts as a barrier between the shock waves produced by detonation, and the static conditions in the air manifold. Without this barrier the shock waves may be preventing consistent air flow into the combustion chamber. Developing a better understanding of what mechanism(s) are causing sub-optimal detonation would be a useful topic for future test campaigns.

Achieving detonation without encountering a substantial pressure loss at the inlet marked an important achievement in the program. In all other tests the negative effects discussed above disallowed the formation of sustained detonation behavior under low pressure drop conditions. A combination of the hardware geometries and flow conditions utilized during these tests overcame such conditions and allowed for sustained detonation waves through completely subsonic inlet flow. With regards to system performance, total pressure gain was never actually realized, even in the low pressure drop tests. Referring back to Table 3, however, the best pressure recovery seen during the entire campaign was realized using low pressure loss inlet hardware. Achieving sustained detonation while avoiding a substantial pressure loss at the inlet was the largest contributor to improving system performance in this test campaign.

Given the frequency and velocity of the waves, the possibility of acoustic mode waves should be discussed CEA was run with propellants and pressures similar to these cases and the hot gas sonic velocity is 989 m/s for the *hp* (deflagration constant pressure) case in test 2 and 993 m/s in test 4. With the wave velocity only slightly above the hot gas sonic velocity, acoustic modes would again be possible. Also note that the unburnt, mixed fill gases have an estimated sonic velocity of 529 m/s and 534 m/s respectively so from that reference frame, the waves are travelling Mach 2.0+ with 56% of CJ velocity. Figure 9 can be compared to Figure 10 in considering acoustic wave shapes to those measured during the low pressure drop testing.

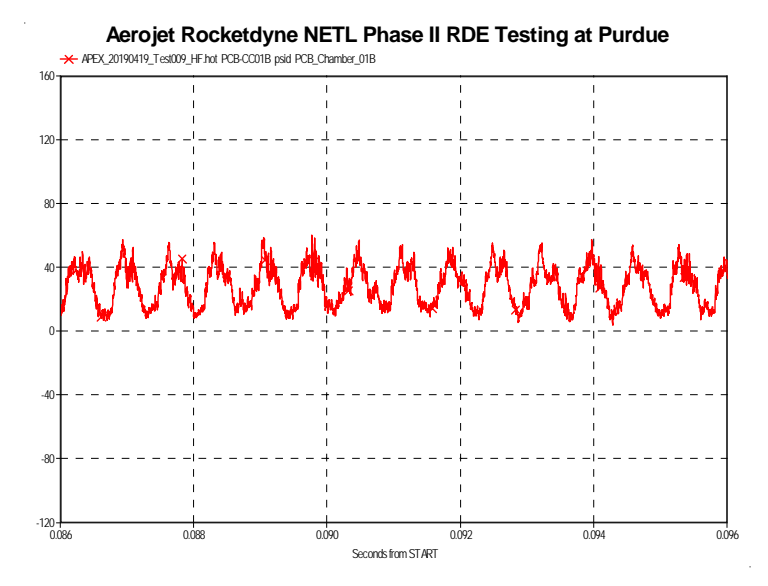


Figure 10 Example of pressure traces produced by transverse acoustic waves passing through an engine.

D. Low Equivalence Ratio Detonation

The testing that occurred on 4/23 provided some interesting and unexpected results. During test 6 and test 9 the fuel injection was tailored in a deliberate manner unlike the rest of the campaign. The result was fuel injection into the system at an equivalence ratio substantially lower than any other test. These conditions produced sustained, one directional waves in both test cases. For all other tests in the campaign, when injection was uniform across the mixing zone, detonation behavior ceased below a minimum equivalence ratio of around 0.9 or higher. These low equivalence ratio tests also used the same low pressure loss hardware configurations as the testing on 4/3. The same low pressure drop phenomenon was observed, including the lack of a choke point used to amplify fuel mixing. For these reasons, the active theory is that a tailoring of the detonation behavior was occurring through the annulus. One region of air flow mixed effectively with the injected fuel to an equivalency ratio of approximately 1. The detonation wave passed through this region of flow no different than under nominal RDE conditions. A second region of air flow avoided substantial mixing with the injected fuel and thus did not combust in the chamber. Instead it flowed through the annulus and mixed with the exhaust products of the detonation process prior to exiting the engine. Another interesting observation during disassembly of the engine was that no scorch or heat marks were seen upstream of the inlet throat where fuel was being injected. This indicates, although doesn't confirm, that the detonation behavior was occurring downstream of the injection point and downstream of the inlet throat. This was unexpected, as the test utilized the same inlet hardware as the low pressure drop testing. Assuming airflow remained subsonic throughout the inlet, one would expect detonation processes to travel upstream to the fuel injection point. This phenomenon is of particular interest in potential future test campaigns. Characterization of the detonation behavior during these tests can be seen below.

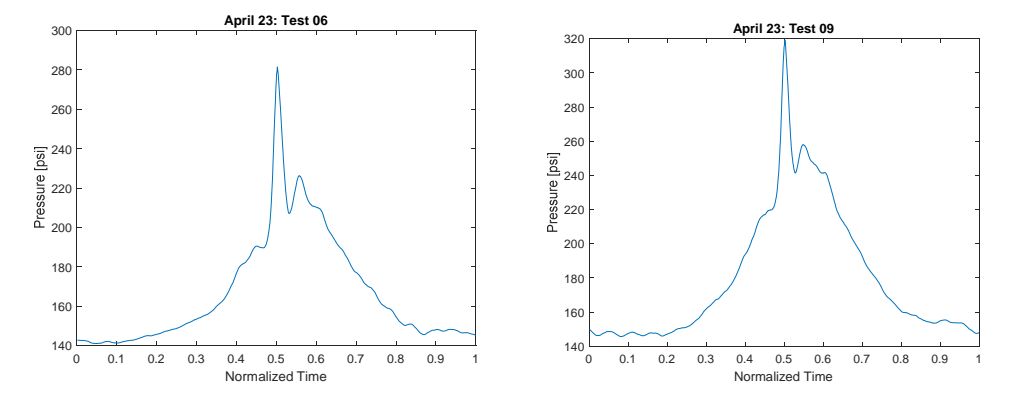


Figure 11 The average shape of the pressure cycle as a detonation wave passes by a PCB during the low pressure loss testing on 4/23. This is an average of all waves over a 0.1 second period.

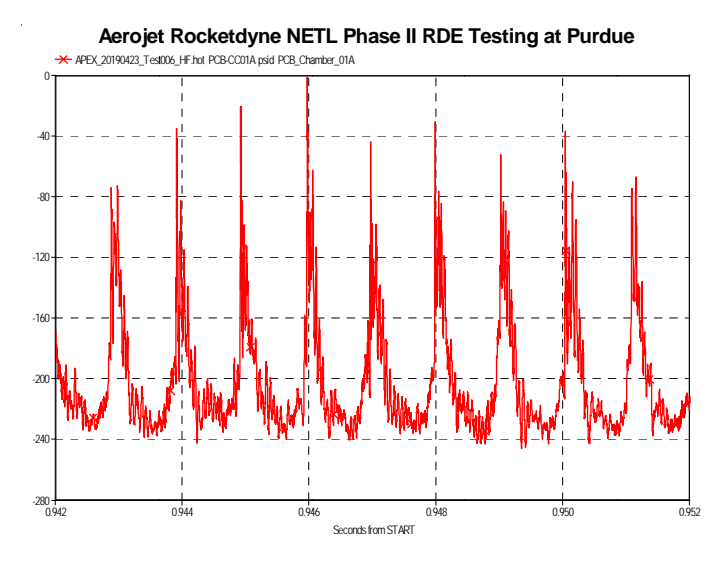


Figure 12 Raw pressure data of detonation waves measured during test 6 on 4/23. Wave traces measured during test 9 on 4/23 are comparable.

Figure 11 and Figure 12 shows the averaged and raw pressure traces of the detonation waves measured during the low equivalence ratio testing. Like the low pressure drop testing, the traces are not traditionally what would be expected from detonation waves. Although there is a sharp peak, the wide base indicates substantial deflagration behavior in the engine.

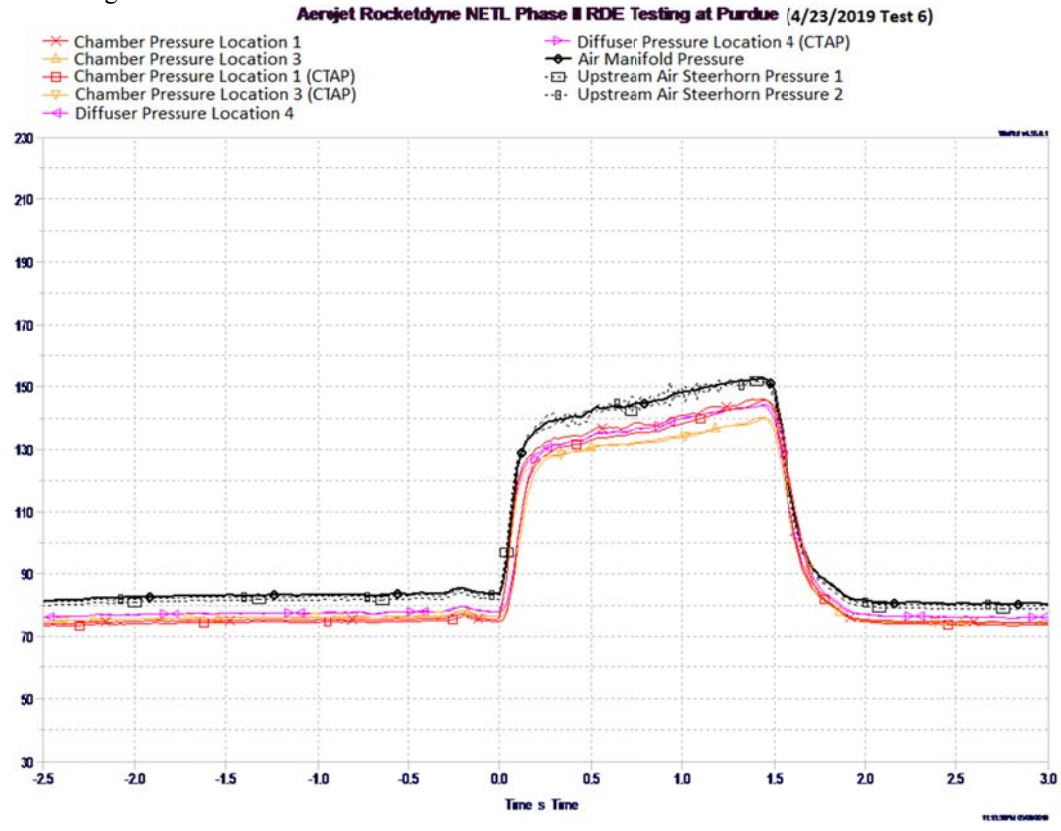


Figure 13 Plotted traces of the low speed pressure sensors during test 6 on 4/23. The trace for test 9 on 4/23 is similar in shape.

Figure 13 displays a static pressure trace measured from the test article during a low equivalence ratio testing. As seen previously, the small gap between the manifold and the chamber indicated a low pressure loss inlet. The

pressure loss between the air manifold and the chamber was measured at less than 7% during low equivalence ratio testing.

Table 7 Characteristics of measured detonation waves during the low pressure loss testing on 4/23.

*Peak measurements with previously described aperture.

Date	Test #	Chamber Pressure (psi)	*Average Peak (psi)	*Average Peak to Satic Pres. Ratio	Dominant Freq (Hz)	Number of Waves	Wave Speed (m/s)	Ratio Actual to CJ Velocity
4/23/2019	006	145	191	1.31	970	1	1037	55.9%
4/23/2019	009	156	230	1.47	1030	1	1101	58.1%

As before, the possibility of acoustic mode waves should be discussed for the low equivalence ratio tests. CEA was run with propellants and pressures similar to these cases and the hot gas sonic velocity is 936 m/s for the *hp* (deflagration constant pressure) case in test 6 and 955 m/s in test 9. With the wave velocity only slightly above the hot gas sonic velocity, acoustic modes would again be possible. Also note that the unburnt, mixed fill gases have an estimated sonic velocity of 549 m/s and 536 m/s respectively. So from that reference frame, the waves are travelling Mach 2.0+ with 56% and 58% of CJ velocity. Figure 12 can be compared to Figure 10 in considering acoustic wave shapes to those measured during the low equivalence ratio testing.

The overall goal of the program was to evaluate the benefits of an RDE in a turbine power plant system. The goal of this test campaign was to identify significant measurements that could be applied to ground a complete RDE power plant system model to evaluate overall performance. The RDE power plant efficiency would then be compared to the efficiency of existing turbine systems. In this analysis, additional benefits were found from the tailored flow phenomenon. The tailored flow model saw a notable increase in efficiency when compared to the traditional RDE model.

IV. Conclusion

The overall goal of the DOE/NETL funded program was to evaluate the benefits of an RDE in a turbine power plant system. Subcontracted efforts led by AR at Southwest Research Institute, the University of Alabama, the University of Michigan and Purdue University all contributed to the experimental design, diagnostic techniques and test approach for a large engineering scale RDE combustor. The engineering scale engine was designed to be highly modular and take advantage of the capabilities of the Purdue Zucrow Labs test capabilities. The RDE annular combustor dimensions of 13.4" OD and 11.7" ID were selected to be large enough to allow detonation waves to continuously propagate and to keep within the hot air flowrate and pressure capabilities of the test facility. Beginning December 2018 and continuing into May 2019, 195 hot fire tests were conducted with 22 different hardware combinations. Total air and fuel flowrates up to 24 lbm/sec and combustor pressures up to 204 psia were achieved, which is equivalent to an overall pressure ratio (OPR) of approximately 14. Some of the tests used the Purdue 100kHz particle image velocimetry (PIV) capability to measure exhaust velocity vectors and help anchor analytical models.

A few tests utilized an inlet/injector configuration which allowed sustained detonation combustion with less than 7% pressure loss from manifold to combustor. Also, a tailored injection scheme allowed overall detonation combustor operation with a low fuel equivalence ratio.

While many of the tests with various hardware configurations were used for analytical model validation and understanding of RDE operability with natural gas, data from the low inlet delta pressure and low fuel equivalence tests were used to baseline combustor capability in a power plant system study. Figure 14 shows a schematic of the plant system used to estimate net efficiency using a pressure gain combustor. The integration of a RDE combustor array between the main air compressor and the turbine was simulated in a manner wherein all the air flows through the combustor without the use of a bypass system. The tailored flow and low equivalence ratio configuration is what allows elimination of the air bypass, which also eliminates the air mixer, a likely source of total pressure loss.

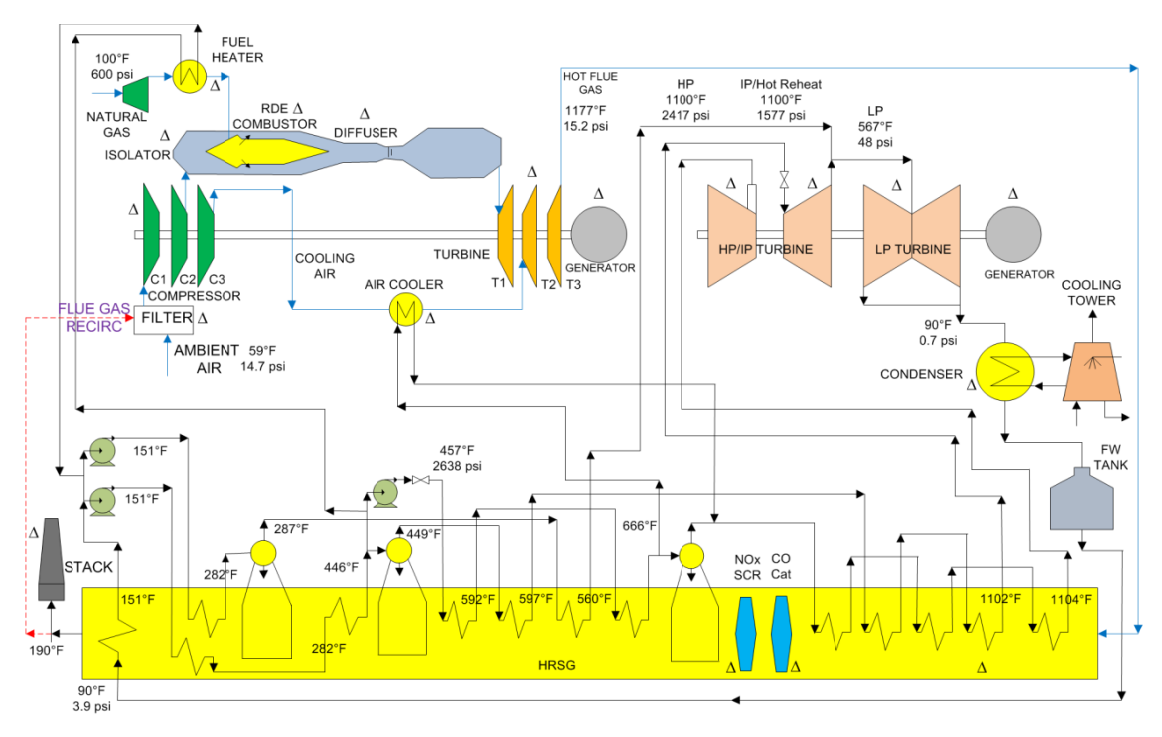


Figure 14. Schematic of a natural gas combined cycle plant with low fuel equivalence ratio combustor (no bypss flow, no mixer)

The combustor and diffuser components of the plant system model were simulated using ChemCAD. Figure 15 shows the block diagram of the ChemCAD simulation. The combustion process was set up to allow a combination of detonation combustion and deflagration combustion, which allowed matching of measured data and also coincides with the parasitic and commensurate combustion observed by Gamba et. al. [3].

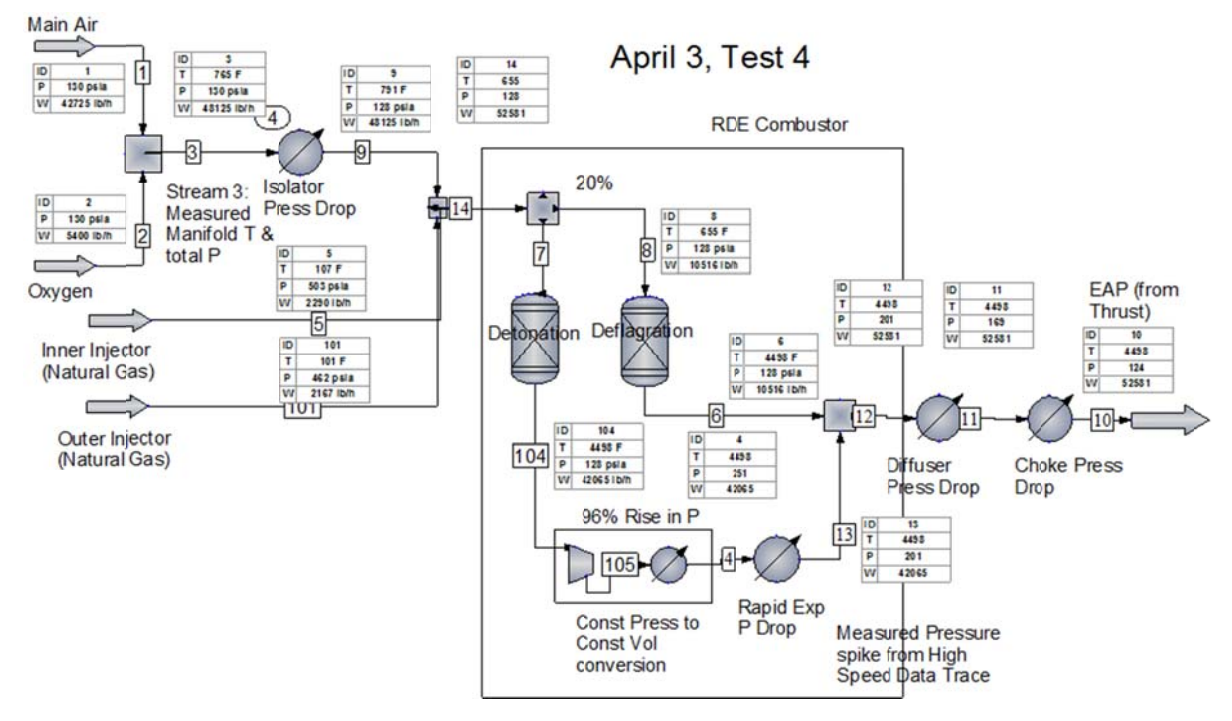


Figure 15. ChemCAD Simulation of test 4 carried out on April 3, 2019

In order to simulate the pressure gain combustion, the measured data from hot fire tests was first simulated to get an idea of efficiency and pressure drop across individual units. Both tailored and uniform combustion cases were simulated. Anchoring points included EAP (from thrust measurement), input flow rate, temperature and pressure of natural gas, air and oxygen as well as measured peak pressure from high frequency pressure data. The final RDE based natural gas power plant had an efficiency of 66.4%.

Acknowledgements

This material is based upon work supported by the Department of under Award Number(s) DE-FE0023983.

Disclaimer: This report was prepared as an account of work sponsored by an agency of the United States Government. Neither the United States Government nor any agency thereof, nor any of their employees, makes any warranty, express or implied, or assumes any legal liability or responsibility for the accuracy, completeness, or usefulness of any information, apparatus, product, or process disclosed, or represents that its use would not infringe privately owned rights. Reference herein to any specific commercial product, process, or service by trade name, trademark, manufacturer, or otherwise does not necessarily constitute or imply its endorsement, recommendation, or favoring by the United States Government or any agency thereof. The views and opinions of authors expressed herein do not necessarily state or reflect those of the United States Government or any agency thereof.

References

- [1] Paxson, D. E., Kaemming, T., "Determining the Pressure Gain of Pressure Gain Combustion," AIAA 2018-4567, July, 2018.
- [2] Bedick, C., Sisler, A., Ferguson, D., Strakey, P., Nix, A., Billips., "Development of a Lab-Scale Experimental Testing Platform for Rotating Detonation Engine Inlets," AIAA 2017-0785, Jan., 2017.
- [3] Chacon, F., Gamba, M., "Study of Parasitic Combustion in an Optically Accessible Continuous Wave Rotating Detonation Engine," AIAA 2019-0473, Jan., 2019.